ACADEMIC
PRESS

reg6 is required for branching morphogenesis during blood vessel regeneration in zebrafish caudal fins

Cheng-chen Huang,[a] Nathan D. Lawson,[b] Brant M. Weinstein,[b] and Stephen L. Johnson[a,*]

[a] *Department of Genetics, Washington University Medical School, St. Louis, MO 63110, USA*
[b] *Unit on Vertebrate Organogenesis, NIH, Bethesda, MD 20892, USA*

Abstract

Postnatal neovascularization is essential for wound healing, cancer progression, and many other physiological functions. However, its genetic mechanism is largely unknown. In this report, we study neovascularization in regenerating adult zebrafish fins using transgenic fish that express EGFP in blood vessel endothelial cells. We first describe the morphogenesis of regenerating vessels in wild-type animals and then the phenotypic analysis of a genetic mutation that disrupts blood vessel regeneration. In wild-type zebrafish caudal fins, amputated blood vessels heal their ends by 24 h postamputation (hpa) and then reconnect arteries and veins via anastomosis, to resume blood flow at wound sites by 48 hpa. The truncated vessels regenerate by first growing excess vessels to form unstructured plexuses, resembling the primary capillary plexuses formed during embryonic vasculogenesis. Interestingly, this mode of vessel growth switches by 8 days postamputation (dpa) to growth without a plexus intermediate. During blood vessel regeneration, vessel remodeling begins during early plexus formation and continues until the original vasculature pattern is reestablished at ~35 dpa. Temperature-sensitive mutants for *reg6* have profound defects in blood vessel regeneration. At the restrictive temperature, *reg6* regenerating blood vessels first fail to make reconnections between severed arteries and veins, and then form enlarged vascular sinuses rather than branched vascular plexuses. Reciprocal temperature-shift experiments show that *reg6* function is required throughout plexus formation, but not during later growth. Our results suggest that the *reg6* mutation causes defects in branch formation and/or angiogenic sprouting.
© 2003 Elsevier Inc. All rights reserved.

Keywords: Zebrafish; Regeneration; Angiogenesis; Plexus; Branching; Anastomosis

Introduction

The genetic control of blood vessel growth and patterning is crucial for both normal development and tumor progression. Understanding the genetic mechanisms that control vessel growth and patterning should enhance our ability to combat inherited vascular diseases and cancer (Hanahan and Folkman, 1996). Blood vessels grow by vasculogenesis (de novo development of the vasculature) and angiogenesis (review by Risau, 1997).

Angiogenesis is the growth of blood vessels from existing vessels (Risau, 1997). In embryos, it replaces vasculogenesis as a mode of vessel growth and morphogenesis after

the formation of the primary capillary plexus (Conway et al., 2001). This mode continues throughout embryogenesis to pattern the mature vasculature. In adults, most vascular endothelial cells are nonmitotic, but can be induced by certain physiological and pathological conditions to enter the cell cycle and grow. For instance, neovascularization is induced in the uterus and ovary during the female reproductive cycle (Reynolds et al., 1992) and in tumor growth (Hanahan and Folkman, 1996). Mechanisms of angiogenesis serve to generate the proper amounts of vessels for target tissues as well as to model vessels into correct patterns. These mechanisms involve several complex cellular processes and interactions, including cell division for vessel growth, sprouting to generate vessel branches, cell migration and guidance for proper routing between vessels and tissues, and cell fusion or retraction (and possibly other

---

* Corresponding author. Fax: +1-314-362-7855.
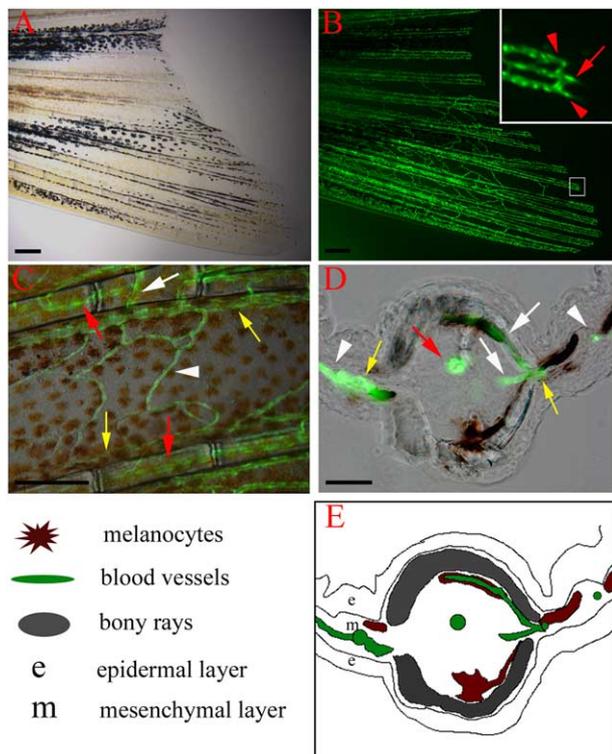*E-mail address:* sjohnson@genetics.wustl.edu (S.L. Johnson).

Fig. 1. Vasculature of the zebrafish caudal fin. *TG(fli1:EGFP)^{y1}* fish express EGFP in blood vessel endothelial cells. (A) Bright field image of the ventral half of the caudal fin of an adult *TG(fli1:EGFP)^{y1}* fish and (B) epiflourescence image of the same fin, revealing the vasculature. (Inset) Higher magnification of the distal end of a fin ray (boxed region) shows that each fin ray is associated with one artery (red arrow) in the center of the ray and two veins (red arrows) adjacent to the bony ray. (C) High magnification image shows the intervessel commissures within the same ray (white arrow), which connect artery to vein as well as vein to vein. The interray vessels (white arrowhead) connect vein to vein of adjacent rays. (D, E) Cross-section through a fin ray shows the artery in the center of intraray mesenchyme (red arrow), while the veins are in interray mesenchyme adjacent to the bony rays (yellow arrows). Intervessel commissures (white arrows) and interray vessels (white arrowheads) are also visible in this section. Explanatory diagram is shown in (E). Scale bars, 200 μm in (A, B, C), 20 μm in (D).

the mesenchymal layer include fibroblasts, blood vessel endothelial cells, axons and glial cells, osteoblasts, osteoclasts, and pigment cells. This simple cellular composition and organization is well suited for studying the regeneration of particular cell or tissue types. Fin regeneration follows the stereotypical sequence of events for epimorphic regeneration (Johnson and Weston, 1995). In brief, during wound healing, lateral epidermal epithelia migrate to cover the stump within 12 h postamputation (hpa). The intraray mesenchymal cells then are induced to enter the cell cycle
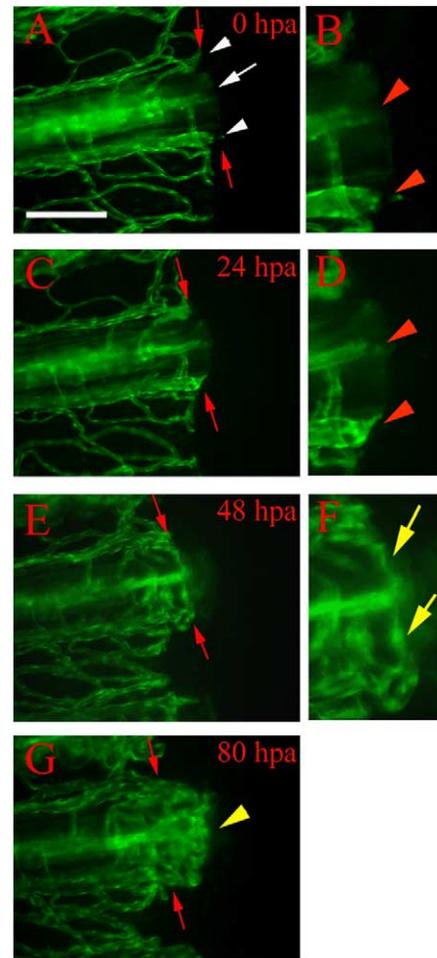

Fig. 2. Vessel healing and anastomosis. Time-lapse images from a representative regenerating fin ray of *TG(fli1:EGFP)^{y1}* show healing and anastomosis of amputated blood vessels during early regeneration. (A) After amputation (0 hpa), severed vessels exhibit openings at the amputation plane (white arrow, artery; white arrowheads, veins). (B) Higher magnification of the distal ends of the severed vessels in (A) show the openings (red arrowheads). (C) These vessels are sealed by 24 hpa (note rounded ends) and sprouts (arrowheads) are frequently observed in (D) enlarged image of the amputation plane. (E) By 48 hpa, cut ends of blood vessels have formed anastomotic bridges between the artery and veins within the same fin ray. Blood flow has resumed through these bridges by this stage (not shown). (F) Higher magnification of the reconnected vessels of (E) shows anastomotic bridges connecting the artery and the two veins (yellow arrows). (G) By 80 hpa, we observe new blood vessels sprout from the distal face of anastomotic bridges (yellow arrowhead). Red arrows point to amputation plane. Diffuse green is autofluorescence from fin ray (possibly bone matrix). Scale bar, 100 μm.

mechanisms) for pruning. Furthermore, during angiogenesis, the interactions between vascular endothelial cells and other mesenchymal cells, mainly smooth muscle cells and pericytes, also play important roles in vessel maturation and stabilization (Carmeliet, 2000). Together, these intrinsic and extrinsic cellular mechanisms shape the arteries and veins to form the final vascular pattern (Risau, 1997).

Zebrafish have become a powerful genetic tool for studying vertebrate development in recent years. The simple cellular composition of the caudal fin (Becerra et al., 1983) and the ability of fish to regrow fins following amputation provide a useful tool for exploring the genetic and cellular mechanisms for tissue regeneration (Johnson and Weston, 1995; Johnson and Bennet, 1999). The zebrafish caudal fin is composed of 18 bony fin rays. Two major cellular compartments are found in the fin ray: the central mesenchymal layer and the overlaying epidermal epithelia. Cell types in
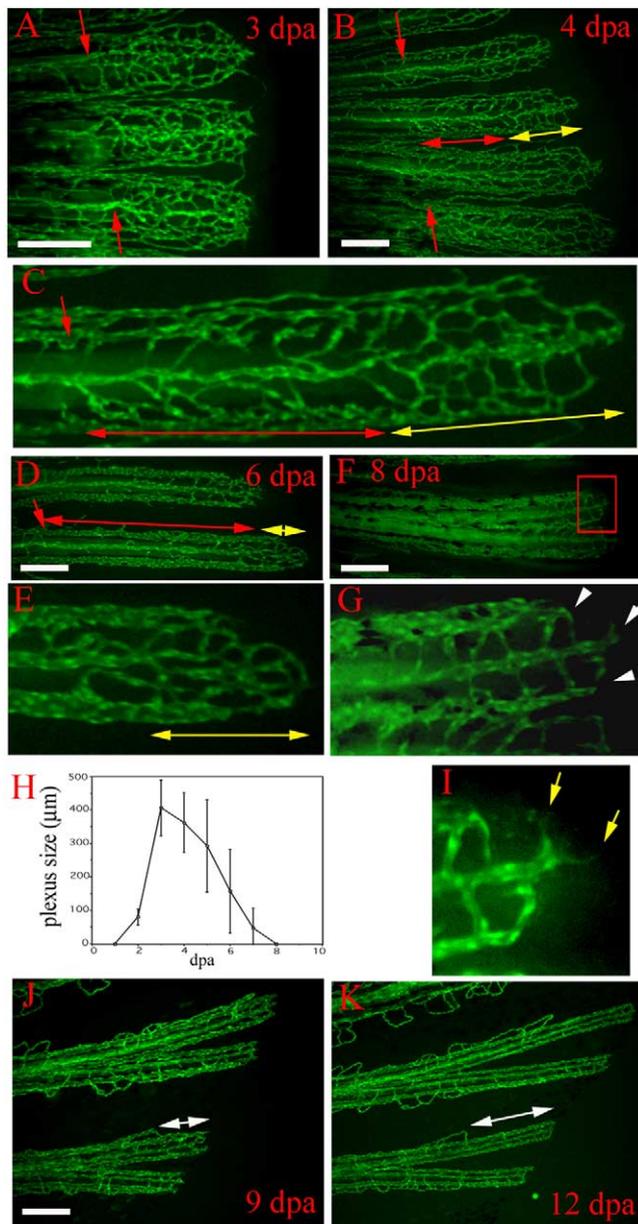
Fig. 3. Vasculature plexus formation, plexus remodeling, and late regenerative angiogenesis. Regenerating blood vessels in wild-type *TG(fli1: EGFP)^y1* form plexuses. (A) In 3-dpa regenerates, the regenerating vasculature of each fin ray (three fin rays are shown) consists of a plexus with dense unstructured vessels extending distally from the amputation plane (red arrows). (B) By 4 dpa, the plexus is remodeled into distinguishable arteries and veins in the proximal regenerate (region delineated by red double-headed arrow). A vasculature plexus is still present at the distal end (region delineated by yellow double-headed arrow). Higher magnification of one fin ray of this regenerate is shown in (C). (D) Coincident with plexus remodeling, the plexus becomes smaller (region delineated by yellow double-headed arrow in D and E) in later regenerates as shown in a 6-dpa regenerate. Higher magnification of the delineated plexus in (D) is shown in (E). (F) Low magnification and (G) high magnification of the distal end of an 8-dpa regenerate show that the plexus has been entirely remodeled into arteries (white arrow in G) and veins (white arrowheads in G). (H) The plexus length (as denoted by yellow double-headed arrows in B–E) reaches a maximum of 400–500 μm at 3 dpa and disappears by 8 dpa. After 8 dpa, vessel growth proceeds by sprouting angiogenesis without a plexus inter-mediate, which we refer to as late regenerative angiogenesis. (I) Enlarged

starting at 36 hpa to form the regeneration blastema (Johnson and Bennet, 1999; Poss et al., 2000; Nechiporuk and Keating, 2002). Blastemal cells then undergo active cell proliferation and differentiation during regenerative growth to replace the lost tissue. Blood vessel regeneration in the regenerating fin has not been previously described.

Here, we report studies on blood vessel regeneration in regenerating fins, using *TG(fli1:EGFP)^y1* transgenic zebrafish (Lawson and Weinstein, 2002). This line expresses EGFP in blood vessel endothelial cells throughout normal development and fin regeneration. We first describe the early stages of vessel morphogenesis during fin regeneration, which include vessel healing, anastomosis to reconnect arteries and veins, plexus formation, plexus remodeling, and intervessel pruning. These early events are followed by a transition to late regenerative angiogenesis characterized by vessel growth without a plexus intermediate.

We also used *TG(fli1:EGFP)^y1* to study a temperature-sensitive fin regeneration mutant, *reg6,* that had previously been described (Johnson and Weston, 1995). We found that *reg6* affects blood vessel regeneration in adult zebrafish. *reg6* mutants first fail to reconnect severed arteries and veins during early vessel regeneration at the restrictive temperature. At subsequent stages, few vessel branches arise, resulting in swollen vessels and less elaborate plexuses. Reciprocal temperature-shift experiments reveal that *reg6* is required during plexus formation but not in subsequent regenerative growth. We suggest that *reg6* is required for branching morphogenesis during anastomosis and throughout plexus formation.

Materials and methods

Fish care

Fish handling and breeding were performed according to standard procedures (Westerfield, 1993).

TG(fli1:EGFP)^y1 and *reg6;TG(fli1:EGFP)^y1* fish

The construction of *fli1:EGFP* plasmid and transgenic fish are described elsewhere (Lawson and Weinstein, 2002). To investigate *reg6^j21* phenotypes in regenerating blood vessels, *reg6^j21; TG(fli1:EGFP)^y1* and *reg6^j21; TG(fli1: EGFP)^y1/+* were generated by traditional crosses and used in this study. Both these genotypes behave similarly in all our experiments.

boxed region of the 8 dpa regenerate in (F) shows sprouts (yellow arrows) formed at the distal end of the growing vessel. (J and K) The same regenerating fin rays imaged at 9 dpa and then again at 12 dpa show that regenerating vessels grow without a plexus intermediate. Amputation plane outside field of view. White double-headed arrows denote the distal growing fin ray. Scale bar, 200 μm.

Regeneration, time-lapse, and temperature-shift experiments

Regeneration experiments were performed on caudal fins that were amputated at approximately 50% proximal–distal level. The amputated fish were kept in 1/2 gallon fish tanks (5–10 fish/tank) with 1 l of water, or in individual 250-ml beaker (1 fish/beaker) with 150 ml of water (for time-lapse experiments). Throughout the experiments, fish were deprived of food. At least five fish of each group were used in each experiment. Staging for normal blood vessel regeneration was done at 25°C with $TG(fli1:EGFP)^{y1}$ fish. The phenotypic comparison between $TG(fli1:EGFP)^{y1}$ and $reg6; TG(fli1:EGFP)^{y1}$ was performed on fish challenged to regenerate at 33°C. For the temperature-shift experiments, fish were shifted between 20 and 33°C. The same fin ray and vessels of each fish were photographed at different time intervals during the course of time-lapse and temperature-shift experiments.

Measurement

Measurements were performed on fins of paraformaldehyde fixed fish. Since the results obtained from different fin rays vary, only measurements from the third fin ray from the dorsal or ventral edge (#3 and 16) are compared and presented here. In branched fin rays, only one branch is counted. The regenerate length is measured as the distance between the amputation plane and the tip of the regenerate, including the distal epidermis. The size of a plexus is measured as the distance between the distal end of regenerating vessels and the proximal margin of the plexus as defined by the presence of distinctive arteries and veins in the proximal regenerates (see Fig. 3). The density of intervessel commissures is the number of vessels observed between the artery and its two veins divided by the regenerate length (mm).

Results

The vasculature of the zebrafish caudal fin

We used $TG(fli1:EGFP)^{y1}$ transgenic fish expressing enhanced green fluorescent protein (EGFP) under the control of zebrafish *fli1* promoter to investigate blood vessel regeneration in the regenerating zebrafish caudal fin (Lawson and Weinstein, 2002). The endogenous *fli1* gene is expressed in blood vessel endothelial cells (Brown et al., 2000; Lawson and Weinstein, 2002), and the $TG(fli1:EGFP)^{y1}$ transgenic line recapitulates this expression pattern, including the vasculature of the adult fins (Lawson and Weinstein, 2002; S.L.J., unpublished data). Each fin ray is associated with a central artery and two flanking veins (Fig. 1A and B). Cross sections through fixed fins show that the central artery lies in the intraray mesenchyme, while the flanking veins lie just lateral to the fin ray, in the interray mesenchyme (Fig. 1D

and E). In the distal half of a normal adult fin, intervessel commissures are found every 0.1 mm between the artery and veins within the same ray. Typically, such commissures are found at slightly higher density at more proximal levels. In addition, interray vessels connecting veins of adjacent rays are found every 0.5 mm (Fig. 1C and D).

Blood vessel regeneration in the zebrafish caudal fin

We sought to describe the morphogenesis of regenerating vessels. Descriptions of the anatomy of zebrafish fin regeneration have been reported elsewhere (Santamaria et al., 1996; Johnson and Bennet, 1999; Poss et al., 2000).

I. Vessel healing and anastomosis at the amputation plane

During the first 12 h postamputation (hpa), the severed ends of arteries and veins are apparent as open-ended vessels (Fig. 2A and B), although bleeding terminates during the first hour. Healing of severed blood vessels occurs by 24 hpa, as the vessel ends appear rounded (Fig. 2C and D), suggesting that changes in endothelial cell shape act to close off the severed vessels. These rounded ends (of both arteries and veins) often show additional protrusions or sprouts, presumably as a precursor to reconnection or anastomosis. These sprouts usually extend distally, then turn laterally to grow toward the other vessel ends. Anastomosis between the wounded arteries and veins then ensues between 36 hpa, when none (0/90) of the fin rays examined showed reconnecting bridges, and 48 hpa, when most (80/90) examined fin rays showed reconnecting bridges between arteries and veins (Fig. 2E and F). Anastomoses mostly occur between the artery and veins of the same ray. Rarely, we observe connections between vessels of adjacent rays, but these connections dissociate soon afterwards. Blood flow resumes in all anastomotic bridges by 48 hpa, indicating that these structures are now functional vessels.

II. Plexus formation, plexus remodeling, and late regenerative angiogenesis

Shortly after the anastomotic bridge is made, multiple distally extending sprouts are observed emerging from the distal face of the bridge, leading to formation of a vascular plexus (Fig. 2G). These new branches are thinner than original vessels and make numerous connections with neighboring vessels. There is no clear morphological distinction between arteries and veins in these early regenerating blood vessel plexuses (Fig. 3A). Blood flow is seen in almost all the small vessels in the plexus that have successfully made connections with neighboring vessels. During the course of plexus formation, the unstructured regenerating vessels are gradually pruned back and remodeled to form arteries and veins at more proximal levels. This process is manifest as a more ordered vasculature structure emerges, as evidenced by a thickened central vessel with more intense EGFP fluorescence, which extends from the artery in the stump. Following the remodeling, blood begins

to flow distally in this vessel, confirming its identity as an artery at this stage. Similarly, lateral to the artery, two veins can be discerned morphologically by their appearance as thick vessels (in contrast to the thinner structures in the plexus) and functionally by the proximal flow of blood cells (Fig. 3B–E). By 8 dpa, the basic vein–artery–vein architecture is reestablished and no plexus is present in distal regenerates (Fig. 3F and G). The plexuses grow to the maximum size of approximately 500 μm long at around 4 dpa and gradually decrease until they disappear at 8 dpa (Fig. 3H). The decrease in plexus size is caused in part by the decrease in rate of growth of the regenerate and the decrease in rate of the plexus formation between 3 and 8 dpa, coupled with the remodeling of the plexus from the proximal end. Although the regenerating blood vessels stop plexus formation at 8 dpa, the distal ends are still actively sprouting (Fig. 3I), suggesting continuity of blood vessel regeneration. When regenerates were examined by time lapse beyond the plexus formation stage, growth was indeed observed to continue without a "plexus" intermediate (Fig. 3J and K), suggesting a transition in the mode of vasculature growth at 8 dpa. We refer to this phase of blood vessel growth as late regenerative angiogenesis.

III. Intervessel pruning

During plexus remodeling, intervessel pruning begins to remove excess intervessel commissures during early plexus formation and continues until the normal vasculature pattern is regenerated. In normal fins, there are 8 ± 2 intervessel commissures/mm in the distal half of the fin ray (Fig. 4C). In regenerating fins, the density of intervessel commissures increases to a maximum of 32 ± 8/mm at 4 dpa and slowly decreases to the normal level by approximately 35 dpa (Fig. 4A, B, and D). In contrast, interray vessels, which do not arise from the plexus, never regenerate to a density greater than that of the normal fin (not shown).

The reg6 mutation affects anastomosis and plexus formation

reg6 is a temperature-sensitive mutation that results in blood blisters in regenerating fins at the restrictive temperature (Johnson and Weston, 1995). To understand the role of reg6 in earlier morphogenesis of the regenerating vasculature, we crossed *TG(fli1:EGFP)^{y1}* into the reg6 mutant line. Caudal fins from reg6 mutants bearing the *fli1:EGFP* fusion marker were then amputated and challenged to regenerate at the restrictive temperature. We found that regenerating blood vessels in reg6 mutants indeed form clear enlarged blood vessel lumens (Fig. 5F) that later fill with blood cells to form blisters as regeneration proceeds (Fig. 5G).

To help observe the earliest morphological defects associated with the reg6 mutation, we performed time-lapse experiments to examine blood vessel regeneration in reg6 mutants from 12 h to 3 days postamputation. We found that

regenerating vessels in reg6 mutants show defects in anastomosis and plexus formation. At 33°C, all normal blood vessels have formed anastomotic bridges at the amputation plane by 19 hpa (90/90); by contrast, we found few such bridges in the reg6 regenerates (20/82) (Fig. 5E, and Table 1). (Note that the regeneration rate at 33°C is approximately twice as fast as that at 25°C; Johnson and Weston, 1995). The regenerating vessels in reg6 then grow out by direct extension with fewer sprouts than observed in wild-type vessels. These vessels form swollen lumens by 2 dpa (33°C). They are then filled with blood cells and can easily be perceived without magnification by 3 dpa (Fig. 5G and H). Wild-type *TG(fli1:EGFP)^{y1}* fish never develop swollen vessels in their regenerating fins (33°C).

Temporal requirements for reg6 during blood vessel regeneration

Above, we showed that reg6 mutants have defects in anastomosis and plexus formation. To more precisely determine when reg6 function is required during blood vessel regeneration, we performed reciprocal temperature-shift experiments on reg6 regenerates.

In wild-type fish, we always observe completion of anastomosis prior to the onset of multiple distal sprouting and plexus formation, which seems to suggest two distinct morphogenetic stages of blood vessel regeneration. Accordingly, we first focused on the transition period from anastomosis to plexus formation. Specifically, we asked whether reg6 function is required for both anastomosis and plexus formation. Fins from two groups of identical *reg6;TG(fli1:EGFP)^{y1}* fish were amputated. Fish in the first group (upshift group) were allowed to regenerate at the permissive temperature until anastomosis was complete, then were shifted to the restrictive temperature and the regenerating vessels were examined every 6 h. Fish in the second group (downshift group) were challenged to regenerate at the restrictive temperature (33°C) until 25 hpa, when most vessels in wild-type fish have completed anastomosis. These fish were then shifted down to the permissive temperature (20°C), and the regenerating vessels were examined every 12 h.

To determine whether reg6 function is required for plexus formation, we analyzed the regenerating vessels from the upshift group that had successfully completed anastomosis prior to the shift to the restrictive temperature. Among the 67 reg6 vessels identified with anastomotic bridges, 45 developed swollen vessels 12 h post shift (hps) (Fig. 6). This result indicates that reg6 function is required for plexus formation. We then asked whether the failure of anastomosis in reg6 mutants influences plexus formation after reg6 function is restored. Our results from the downshift experiments show that, among the 40 vessels in reg6 mutants that had not completed anastomosis, 32 (80%) of them were able to form connections distal to the amputation plane (rather than at the amputation plane) and developed
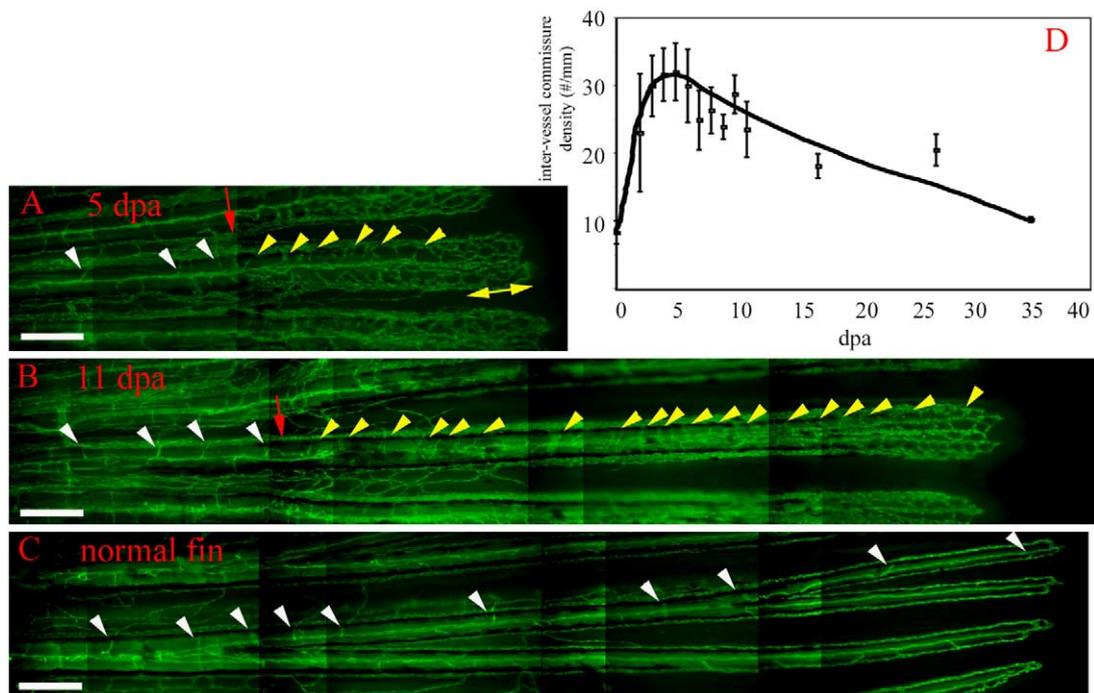
Fig. 4. Intervessel pruning. Following plexus remodeling, the proximal regenerate undergoes intervessel pruning. In 5-dpa (A) and 11-dpa (B) *TG(fli1: EGFP)^{y1}* regenerates, the number of intervessel commissures in the regenerate (yellow arrowheads) is significantly higher than in the stump (white arrowheads) or in the normal fin (C). The yellow double-headed arrow delineates the plexus. (D) Intervessel commissure density in a regenerating fin. Intervessel commissures reach a maximal density at 5 dpa (30 commissures/mm) and are gradually pruned back to the density of a normal fin (~10 commissures/mm, 0 dpa). Scale bar, 200 μm.

normal plexuses following restoration of *reg6* function (Fig. 7). This result suggests that *reg6* function is sufficient to promote normal plexus formation during blood vessel regeneration, even when anastomosis is delayed. We conclude that *reg6* function is required for both anastomosis and plexus formation.

reg6 mutants show defects in vessel branching but not in endothelial cell proliferation

To further understand the cellular basis for *reg6* phenotypes, we next tested the hypothesis that swollen vessels in *reg6* mutants might be due to overproliferation of endothelial cells. Accordingly, we counted the total number of endothelial cells in 2-dpa (33°C) regenerating vessels of wild-type *TG(fli1:EGFP)^{y1}* and *reg6;TG(fli1:EGFP)^{y1}* fish. The cell number was determined in whole-mount regenerates, taking advantage of the fact that EGFP flourescence is more intense in the thickened region of the endothelial cell nuclei (as confirmed with DAPI flourescence, not shown) than in the cytoplasm of the endothelial cells. In wild-type fins that were allowed to regenerate for 2 days (33°C), we found that for the longest fin rays (#3 and 16) there were an average of 220 ± 54 vessel endothelial cells/fin ray in the regenerating vessels distal to the amputation plane (Table 1). For *reg6* mutants under the same conditions, we found no significant difference in the number of vessel endothelial

cells in 2-day regenerates (242 ± 55/fin ray). Therefore, we conclude that the swollen vessels in *reg6* mutants are not the consequence of overproliferation of blood vessel endothelial cells.

We also tested whether swollen vessels result from enhanced growth of one vessel type at the expense of another. If this were the case, we would expect to find swollen vessels more frequently in either arteries or veins. Thus, we examined the frequency of swollen vessels in arteries and veins of 2-dpa and 3-dpa *reg6* regenerates. The results (Table 1) show a similar frequency of swollen vessels in regenerating arteries 45% (36/80) and veins 41% (66/160) of 2-dpa *reg6* regenerates at the restrictive temperature. The frequency of swollen vessels was slightly higher in 3-dpa *reg6* regenerates, but again there was no significant difference between the frequency in arteries and veins (Table 1). Together, these data indicate that the swollen vessel phenotype is not a consequence of overproliferation of endothelial cells or preferential growth of one of the vessel types. Furthermore, we observed that the distance between endothelial cell nuclei in swollen vessels is roughly the same as in normal vessels (note spacing between green foci in the *reg6* swollen vessels is the same as in normal vessels, insets in Fig. 5G and C, respectively). This suggests that *reg6* swollen vessels are not the result of vessel dilation.

Finally, we sought to determine whether the swollen vessels are due to branching defects. By following the
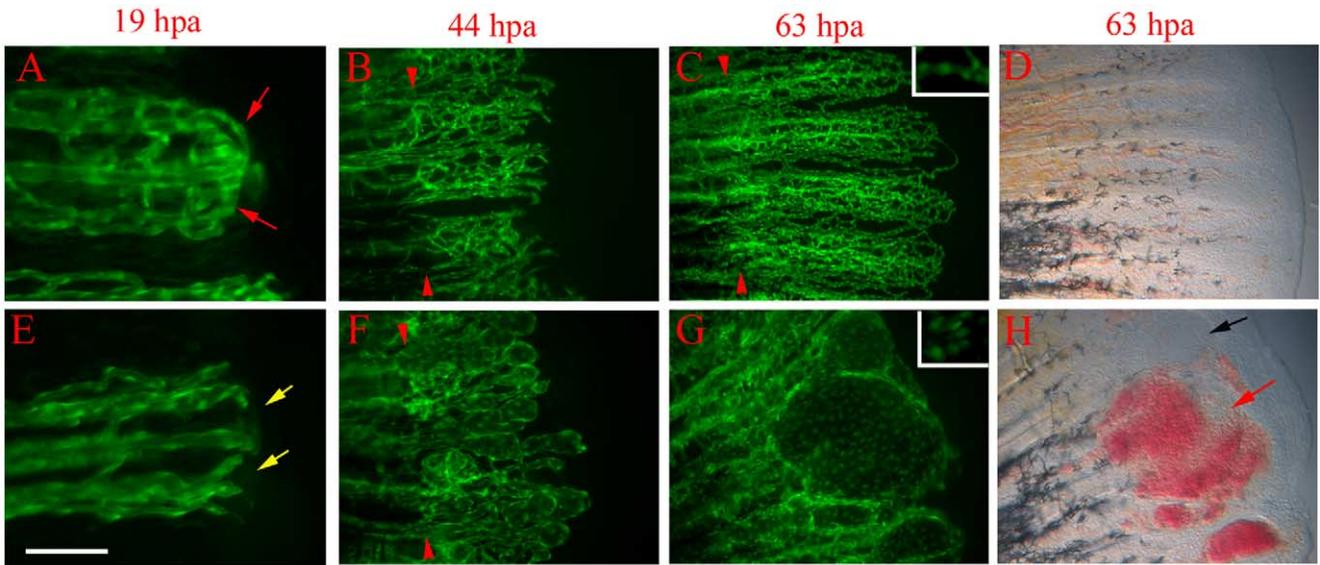
Fig. 5. *reg6* mutants have defects during anastomosis and plexus formation. Time-lapse images of wild-type *TG(fli1:EGFP)*[y1] (A–D) and *reg6;TG(fli1: EGFP)*[y1] (E–H) regenerates show that *reg6* regenerates fail to complete anastomosis before outgrowth and later fail to form plexuses during blood vessel regeneration. (A) and (E) show 19-hpa regenerates (33°C) at which stage the wild-type regenerates (A) have finished anastomosis (red arrows), while *reg6* regenerates failed to do so (E, yellow arrows). By 44 hpa (33°C), the regenerating vessels form plexuses in wild-type regenerates (B), but those in *reg6* mutants grow out without forming plexuses. Instead, they form blisters with few branches (F). In 63-hpa *reg6* regenerates (33°C), some blisters that developed at the distal ends of regenerating vessels (G) are filled with blood cells (red arrow in H) and some remain clear (black arrow in H), which can easily be perceived in bright field. Similar blisters are typically never seen in wild-type regenerates at the same stages (C, D). Insets in (C) and (G) are higher magnification images to show distance between nuclei (green foci) of endothelial cells in wild-type and *reg6* regenerates, respectively. Red arrowheads point to amputation planes. Scale bar, 100 μm for (A, E); 200 μm for (B, F); 300 μm for (C, D, G, H).

development of swollen vessels in *reg6* mutants closely, we found that, at the onset of vessel outgrowth in *reg6* mutants, vessels make few branches. Furthermore, these vessels form small bulbs at their distal ends by 24 hpa (33°C, Fig. 8), which are not seen in wild type (Fig. 2E and G). As these *reg6* vessels grow distally, they continue to swell and the deficit in branching persists through later stages of regeneration. While normal plexuses contain 9 ± 3 branches by 40 hpa (33°C), plexuses in *reg6* mutants contain only 4 ± 2 branches (Table 1). This difference continues through 3.5 dpa (33°C) (36 ± 4 in wild type vs. 17 ± 5 in *reg6* mutants). We also noticed that the *reg6* regenerating vessels with larger blisters tend to have fewer branches (not shown). Together, these observations suggest that the primary defect

in *reg6* mutants is in vessel branching morphogenesis, which leads to formation of swollen vessels.

reg6 function is not required for late angiogenic growth

We next asked whether *reg6* function is required for late regenerative angiogenic growth. To address this question, we performed temperature shifts following completion of plexus formation. In these experiments, *reg6* regenerating vessels were allowed to develop at the permissive temperature through plexus formation and were then shifted to the restrictive temperature during late regenerative angiogenic growth. Among the 42 fin rays examined, none developed swollen vessels in the ensuing 6 days after shift. Therefore,

Table 1
Quantitative morphogenetic analysis of *reg6* phenotype

Genotype	Anastomoses (%)[a]	Cell number[b]	Swollen vessels (%)				Branches[e]	
			2 dpa		3 dpa			
			A[c]	V[c]	A[d]	V[d]	40 hpa	85 hpa
wild type	100 (90/90)	220 ± 54	0	0	0	0	9 ± 3 (25)	36 ± 4 (12)
reg6	24 (20/82)	242 ± 55	45	41	61	63	4 ± 2 (27)	17 ± 5 (19)

[a] Successful formation of anastomotic bridges in individual fin rays by 19 hpa at 33°C.
[b] EGFP-positive endothelial cells/fin ray, distal of amputation plane in 2 dpa regenerates at 33°C ($n = 5$ fins).
[c] At 33°C, $n = 80$ arteries (A) and 160 veins (V).
[d] At 33°C, $n = 98$ arteries (A) and 196 veins (V).
[e] Per plexus, at 33°C. Number in parenthesis indicates number of plexuses examined.
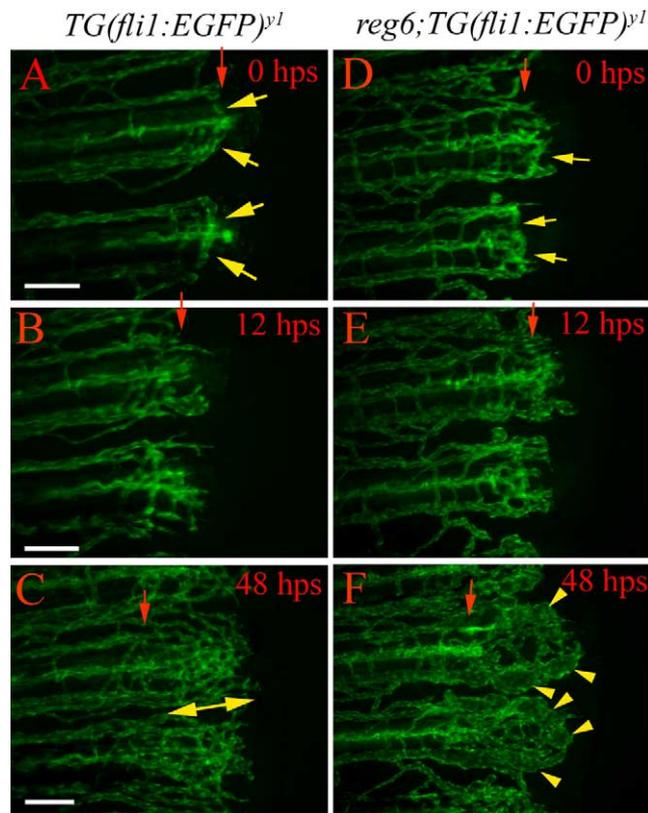
Fig. 6. *reg6* function is required for plexus formation. In the temperature up-shift experiment, wild-type *TG(fli1:EGFP)^y1* (A–C) and *reg6;TG(fli1: EGFP)^y1* (D–F) fish were allowed to complete anastomosis at the permissive temperature (20°C) and were then shifted to the restrictive temperature (33°C). In wild-type animals, the regenerating vessels form anastomotic bridges at the time of shift (A). By 12 h postshift (hps), multiple distally extending sprouts grow out from the distal face of the anastomotic bridges (B). The regenerating vessels in wild-type animals develop normal plexuses 48 h after shift to the restrictive temperature (C). In contrast, although the regenerating vessels in *reg6* mutants had successfully completed anastomosis at the time of shift (D, regenerates shifted at 77 hpa are shown), they developed swollen vessels within 2 days at the restrictive temperature (F). hps, hour post shift. Red arrows, amputation plane; yellow arrows, anastomotic bridges; yellow arrowheads, swollen vessels; double-headed arrow, plexus. Scale bar, 100 μm.

we suggest that *reg6* function is not required for late angiogenic growth.

reg6 is required for branching morphogenesis in developing embryos

We previously described the formation of sinuses in developing *reg6* embryos at the restrictive temperature (Johnson and Weston, 1995). We wondered whether this embryonic phenotype in *reg6* mutants also results from branching defects in endothelial cells. To test this, we performed time-lapse experiments to examine the developing vasculature in *TG(fli1:EGFP)^y1* and *reg6;TG(fli1:EGFP)^y1* embryos at the restrictive temperature. We found that *reg6* embryos are able to develop vasculature normally except for

the caudal vein. In wild-type zebrafish embryos, the dorsal aorta and cardinal vein grow posteriorly to form caudal aorta and vein, respectively (Isogai et al., 2001). The developing caudal veins first grow numerous branches and then form plexuses before they are remodeled into a single caudal vein by 5 days postfertilization. In our time-lapse experiments, developing caudal veins in *reg6* embryos form fewer branches and develop large sinuses at the restrictive temperature (Fig. 9), in a phenotype analogous to that seen in adult regenerating vessels. Thus, we conclude that *reg6* function is required for branching morphogenesis in the developing caudal veins during embryogenesis as well as in adult regenerating vessels. In contrast to high penetrance (~100%) of the *reg6* phenotype in regenerating fins, the penetrance of the embryonic phenotype is much lower, typically 5% (C-C.H. and S.L.J., unpublished data).
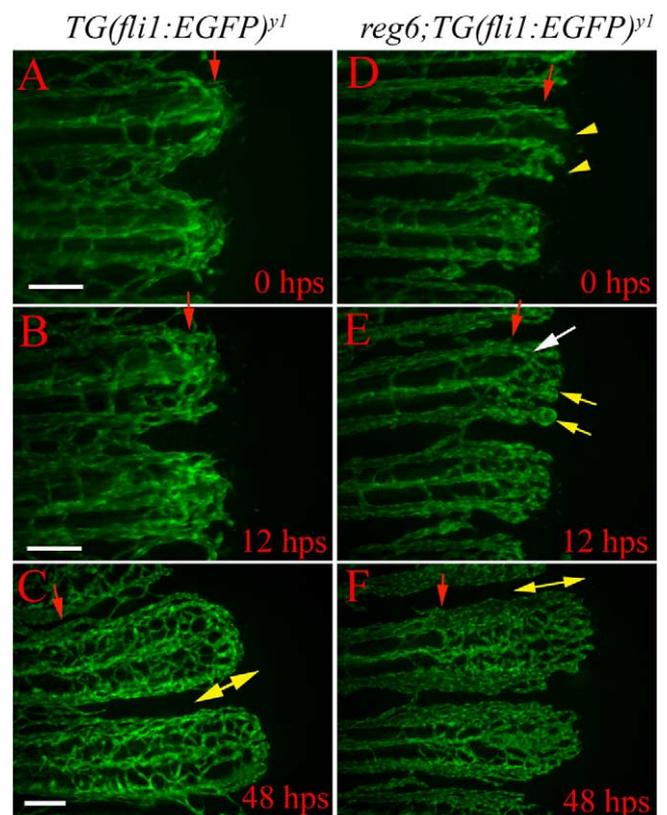

Fig. 7. Temperature down-shift experiments show that anastomosis can be delayed with no apparent consequence to the plexus formation. While wild-type fish (A–C) always complete anastomosis successfully and develop normal plexuses in these experiments, most regenerating vessels in *reg6* mutants (D–F) had failed to complete formation of anastomotic bridges (D) at the time of shift (26 hpa) (yellow arrowheads point out the absence of anastomotic bridge at amputation plane; also see Table 1). (E) Although the vessels developed small bulbs at the distal ends (yellow arrows), they were able to form anastomotic bridges at a more distal position (white arrow) 12 hps. (F) These vessels developed normal plexuses within 2 days after shift to the permissive temperature. hps, h postshift. Red arrow, amputation plane; yellow arrow, swollen vessels; double-headed arrow, plexus. Scale bar, 100 μm.
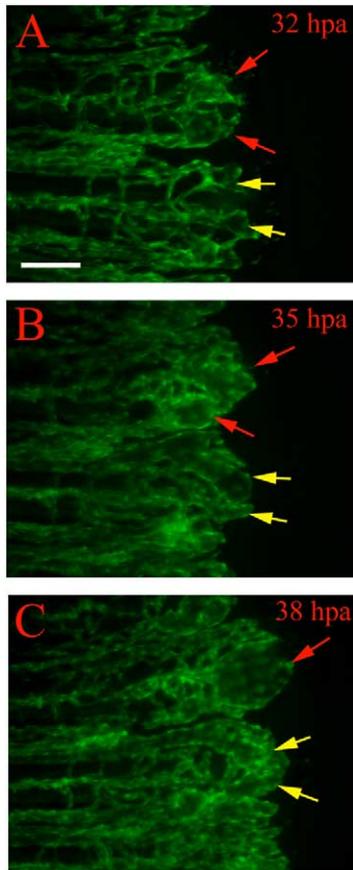
Fig. 8. Regenerating vessels in *reg6* mutants show defects in branching. Time-lapse images from regenerating vessels of *reg6;TG(fli1:EGFP)^{y1}* show defects in branching. (A) At 32 hpa (33°C), the regenerating vessels in *reg6* mutants grow out with few branches and develop small bulbs at distal ends of individual arteries and veins (red and yellow arrows). These bulbs continue to grow through 35 hpa (B) and then form enlarged blisters a few hours later (C, red and yellow arrows) with fewer branches than wild type (also see Table 1). Note vessels denoted by red arrows fuse, while vessels denoted by yellow arrows remain distinct. Scale bar, 100 μm.

Discussion

Stages of blood vessel regeneration

The regeneration of blood vessels in the regenerating zebrafish fin involves the following morphogenetic mechanisms: vessel healing, artery–vein anastomosis, plexus formation, plexus remodeling, intervessel pruning, and late regenerative angiogenesis (Fig. 10). Each stage provides distinct opportunities for investigating morphogenetic mechanisms. A few of them are discussed below.

I. Branching morphogenesis, anastomosis, and plexus formation

After vessel healing, regenerating vessels undergo active branching morphogenesis to accomplish anastomosis and plexus formation. Branches are first observed sprouting from severed vessels by 24 hpa (25°C). Sprouting branches

remain within the same fin ray; sprouts from arteries grow out toward flanking veins and sprouts from veins grow in towards the central artery. Thus, these sprouting branches form two bridges that connect the artery to the adjacent veins, completing anastomosis by 48 hpa (25°C). During anastomosis, veins within the same fin ray never form connections. However, veins may form connections with adjacent rays, albeit rarely. In these instances, we observed dissociation of these aberrant connections soon afterward, raising the possibility that specific recognition signals between arteries and veins within the same ray promote successful anastomosis. Anastomosis is immediately followed by blood flow resumption and formation of additional sprouts that interconnect and elaborate to form a vascular plexus. The fact that blood flow resumes in the reconnected vessels before outgrowth occurs may also reflect the importance of blood supply for regenerating tissue. These observations in wild-type regenerating vessels suggested that, to facilitate plexus formation, anastomosis must occur at the amputation plane prior to vessel outgrowth. However, our observations in *reg6* show otherwise. In our down-shift experiments, *reg6* regenerating vessels grow out without first completing anastomosis. Furthermore, after *reg6* function is restored, plexuses form normally, despite the delayed onset of anastomosis (Fig. 7). These results indicate that outgrowth of regenerating vessels can occur before anastomosis and that anastomosis can be temporally delayed and
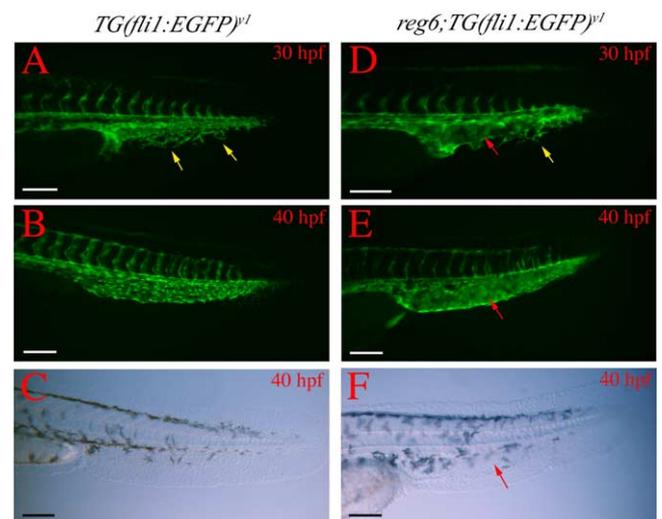

Fig. 9. Branching defects in developing caudal veins in *reg6* embryos. (A) A wild-type *TG(fli1:EGFP)^{y1}* embryo at 30 h postfertilization (hpf) (33°C) shows numerous branches (yellow arrows) in the developing caudal vein. (B) These branches develop into a plexus within a few hours and the plexus persists for several days during embryogenesis (a 40-hpf embryo is shown). (C) Bright field image of (B). (D) The developing caudal vein in *reg6; TG(fli1:EGFP)^{y1}* embryo at 30 hpf (33°C) shows fewer branches (yellow arrow) and a developing sinus (red arrow). (E) By 40 hpf, the developing caudal veins in *reg6;TG(fli1:EGFP)^{y1}* embryos become swollen and form a sinus (red arrow). (F) Bright field image of (E); red arrow, developing sinus. Anterior to the left and dorsal up. hpf, hour post fertilization. Scale bars, 100 μm.
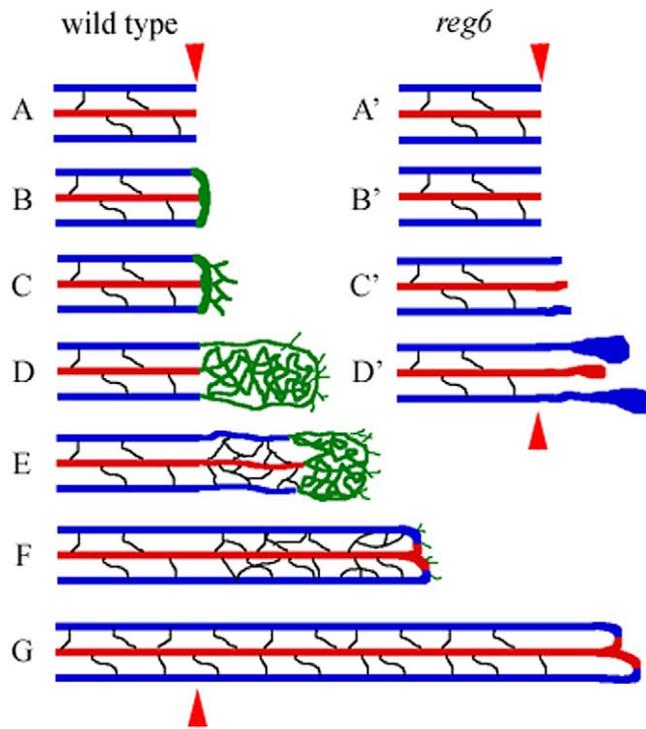
Fig. 10. Summary cartoon of stages of blood vessel regeneration and corresponding *reg6* defects. The red and blue lines depict arteries and veins, respectively. The new vessels in green may or may not yet be specified as artery or vein. Black lines depict inter-vessel commissures. (A) After amputation, the wild type regenerating vessels heal their ends within one day post amputation (dpa). (B) Anastomosis occurs between 1 and 2 dpa. Blood flow to the wound site is restored, and the base for blood vessel regeneration is formed. Soon after anastomosis, blood vessels outgrow to form plexuses (C, D), which are then remodeled from the proximal end into new arteries and veins beginning 1 day later (E). The newly formed arteries and veins appear to have denser intervessel commissures than non-regenerating vessels. New vessels undergo intervessel pruning from 4 dpa onward (E–G). The regenerating blood vessels stop plexus formation at around 8 dpa but continue to grow by late regenerative angiogenesis (F). By around 35 dpa, the density of intervessel commissures has returned to the normal level (G). In *reg6* mutants, wound healing seems to occur normally (A′). However, *reg6* regenerating vessels show defects during anastomosis (B′) and later during plexus formation (C′). The *reg6* regenerating vessels form blisters during plexus formation at the restrictive temperature primarily due to defects in branching morphogenesis (D′). Red arrowhead, amputation plane.

spatially shifted to more distal positions, following return to the permissive temperature.

II. Origin of regenerating blood vessel cells

Our observations of EGFP-labeled cells in regenerating fins suggest that blood vessel growth proceeds by sprouting angiogenesis, where new vessels develop from preexisting vessels. However, our analysis does not firmly exclude the possibility that regenerating blood vessel cells come from undifferentiated cells as well. Such exclusion would require that we track the lineage of all vessel cells in the regenerate back to vessel cells in the stump. Although feasible, we have not yet attempted this. However, evidence from other

experimental systems suggests that vasculogenesis (de novo differentiation of blood vessel cells) may occur in adult vessel growth (Asahara et al., 1997; Shi et al., 1998; Lin et al., 2000; Rafii et al., 1995). Therefore, it remains possible that vasculogenesis also plays a role in vessel regeneration in zebrafish. It has been established that fin regeneration relies on a group of undifferentiated cells, the regeneration blastema, that arises by division of bone and fibroblast cells (and possibly other cell types) at the amputation plane. These blastemal cells then give rise to regenerating tissues (Johnson and Bennet, 1999). Although little is known about cell fate determination in zebrafish fin regeneration, cells in urodele limb and axolotl tail regenerates have been shown to change fates during regeneration (Lo et al., 1993; Echeverri and Tanaka, 2002). In addition, the observation that regenerating pigment cells arise exclusively from undifferentiated precursors (Rawls et al., 2000) seems to support the notion that other regenerating tissues can come from undifferentiated cells. In our experiments, we occasionally observed isolated distal EGFP-positive cells that then joined the growing plexus (not shown), suggesting the possibility that regenerating endothelial cells may arise from undifferentiated blastemal cells. However, our time-lapse observations have shown that, in some of these cases, the EGFP-expressing cells may leave the early plexus, migrate distally, then rejoin the plexus at later stages (not shown), indicating that at least some of these isolated EGFP-positive cells arose from preexisting vasculature. Further experimentation will be needed to determine whether any undifferentiated cells contribute to regenerating vessels.

III. Transition in morphogenetic mechanism of growth

Our analysis of blood vessel regeneration reveals two distinct growth modes, each employing a different mechanism of vessel growth. This differs from fish fin ray growth, which occurs as a reiterated series of morphogenetic events—the episodic addition of fin ray segments (Iovine and Johnson, 2000; Goldsmith et al., 2003). In vascular regeneration, we observed that vessels grow by first forming plexuses. This growth mode persists from 2–8 dpa, at which time they switch to the second growth mode, which we refer to as late regenerative angiogenic growth. During this phase, the regenerating vessels grow by sprouting from their distal ends without forming the plexus intermediate. In addition to the growth-mode transition in regenerating vessels seen at 8 dpa, we also observe a morphogenetic transition at this stage in other regenerating tissue types. Monoclonal antibody 3B12 (S.L.J., unpublished data) recognizes an epitope in a subset of apical epithelial cells beginning at 4 dpa. This expression persists through 8 dpa, at which stage epitope-positive cells are extruded from the fin. Although the nature of 3B12-labeled cells remains unknown, the apparent coincidence of their expulsion with the vasculature transition at 8 dpa suggests that this marks a major transition in the mechanism of fin regeneration. These different growth modes presumably involve different genetic pro-

grams, evidenced by our demonstration that *reg6* mutation profoundly affects the first mode (plexus formation) but not the second mode (late regenerative angiogenic growth). Although late regenerative angiogenesis proceeds without a plexus, it still forms excess numbers of intervessel commissures (Fig. 4B). This high number of intervessel commissures slowly decreases to the wild-type level by 30–35 dpa, suggesting that the entire vessel regeneration program lasts about 1 month (25°C).

Role of reg6 in vessel branching or sprouting

We suggest that the role of *reg6* is to promote branching morphogenesis of the vasculature during regeneration. We were able to exclude the alternative hypotheses of overproliferation of endothelial cells or preferential enhanced growth of one of the two vessel types as responsible for swollen vessel formation in *reg6* mutants. As intensive vessel sprouting and branching occurs during both anastomosis and subsequent plexus formation, we then tested the role of *reg6* function in branching during both events. First, during anastomosis, we observed less sprouting in *reg6* vessels (Fig. 5E) at the restrictive temperature, suggesting that the defect in anastomosis stems from this early defect in branching morphogenesis. A similar branching defect in *reg6* mutants was seen during plexus formation when we shifted fish to the restrictive temperature following successful anastomosis (Fig. 7). Therefore, we conclude that *reg6* function is required for branching morphogenesis in both anastomosis and plexus formation during blood vessel regeneration. Furthermore, we suggest that, in normal regenerating vessels, branches form an outlet for new endothelial cells. Unbranched vessels in *reg6* regenerates fail to provide such an outlet for proliferating endothelial cells. Thus, they become larger and appear swollen.

We suspect that *reg6* mutation primarily affects the morphogenesis of blood vessels, with secondary consequences on morphogenesis of other tissues in the fin or embryo (Johnson and Weston, 1995). For instance, we previously described defects in bone morphogenesis in *reg6* regenerating fins and in epidermis development of ventral fin fold in *reg6* embryos (Johnson and Weston, 1995). Our results described here show that the *reg6* mutation causes profound defects in branching morphogenesis in regenerating vessels, resulting in formation of blood blisters. We also show that the similar branching defects occur in the developing caudal veins in *reg6* embryos (albeit at much lower frequency) followed by formation of sinuses in ventral fin folds. Furthermore, the swollen vessels in both regenerating vessels and developing caudal veins appear prior to other apparent morphological abnormalities, such as thickened epidermis in the developing ventral fin folds and malformed bony rays in regenerating fins (not shown; Johnson and Weston, 1995). These observations using the *TG(fli1:EGFP)^{y1}* to visualize blood vessels now lead us to suggest that the thickened epidermis and malformed bony rays are second-ary consequences of the observed defects in branching, anastomosis and plexus formation, that in turn lead to engorged blood blisters, that by steric means might lead to these other morphogenetic defects.

It remains unclear, however, whether the *reg6* defects in vessel branching, anastomosis and plexus formation are due to cell autonomous defects in the vessel endothelial cells themselves or are the result of defects in signaling events from the surrounding mesenchyme. Cellular autonomy of these defects may be solved by generation of appropriately marked clones in animals chimeric for *reg6,* or alternatively, by positionally cloning the *reg6* gene to generate probes for determining the site of *reg6* gene expression in the regenerating fin.

References

Asahara, T., Murohara, T., Sullivan, A., Silver, M., Van der Zee, R., Li, T., Witzenbichler, B., Schatteman, G., Isner, J.M., 1997. Isolation of putative progenitor endothelial cells for angiogenesis. Science 275, 964–967.

Becerra, J., Montes, G.S., Bexiga, S.R., Junqueira, L.C., 1983. Structure of the tail fin in teleosts. Cell Tissue Res. 230, 127–137.

Brown, L.A., Rodaway, R.F., Schilling, T.F., Jowett, T., Ingham, P.W., Patient, R.K., Sharrocks, A.D., 2000. Insights into early vasculogenesis revealed by expression of the ETS-domain transcription factor Fli-1 in wild type and mutant zebrafish embryos. Mech. Dev. 90, 237–252.

Carmeliet, P., 2000. Mechanisms of angiogenesis and arteriogenesis. Nat. Med. 6, 389–395.

Conway, E., Collen, D., Carmeliet, P., 2001. Molecular mechanisms of blood vessel growth. Card. Res. 49, 507–521.

Echeverri, K., Tanaka, E.M., 2002. Ectoderm to mesoderm lineage switching during axolotl tail regeneration. Science 298, 1993–1996.

Goldsmith, M.I., Fisher, S., Waterman, R., Johnson, S.L., 2003. Saltatory control of isometric growth in the zebrafish caudal fin is disrupted in long fin and rapunzel mutants. Dev. Biol., in press.

Hanahan, D., Folkman, J., 1996. Patterns and emerging mechanisms of the angiogenic swithch during tumorigenesis. Cell 86, 353–364.

Iovine, M.K., Johnson, S.J., 2000. Genetic analysis of isometric growth control mechanisms in the zebrafish caudal fin. Genetics 155, 1321–1329.

Isogai, S., Horiguchi, M., Weinstein, B.M., 2001. The vascular anatomy of the developing zebrafish: an atlas of embryonic and early larval development. Dev. Biol. 230, 278–301.

Johnson, S.L., Bennet, P.J., 1999. Growth control in the ontogenic and regenerating zebrafish fin, in: Detrich IIIH.W., Westerfield, M., Zon, L.I. (Eds.), The Zebrafish Biology, Vol. 59, Academic Press, San Diego, pp. 301–311.

Johnson, S.L., Weston, J.A., 1995. Temperature-sensitive mutations that cause stage-specific defects in zebrafish fin regeneration. Genetics 141, 1583–1595.

Lawson, N.D., Weinstein, B.M., 2002. In vivo imaging of embryonic vascular development using transgenic zebrafish. Dev. Biol. 248, 307–318.

Lin, Y., Weidsorf, D.J., Solovey, A., Hebel, R.P., 2000. Origin of circulating endothelial cells and endothelial outgrowth from blood. J. Clin. Invest. 105, 71–77.

Lo, D.C., Allen, F., Brokes, J.P., 1993. Reversal of muscle differentiation during urodele limb regeneration. Proc. Natl. Acad. Sci. USA 90, 7230–7234.

Nechiporuk, A., Keating, M.T., 2002. A proliferation gradient between proximal and msxb-expressing distal blastema directs zebrafish fin regeneration. Development 129, 2607–2617.

Poss, K.D., Shen, J., Nechiporuk, A., McMahon, G., Thisse, B., Thisse, C., Keating, M.T., 2000. Roles of Fgf signaling during zebrafish fin regeneration. Dev. Biol. 222, 347–358.

Rafii, S., Oz, M.C., Seldomridgem, J.A., Ferris, B., Asch, A.S., Nachman, R.L., Shapiro, F., Rose, E.A., Levin, H.R., 1995. Characterization of hematopoietic cells arising on the textured surface of left ventricular assist devices. Ann. Thorac. Surg. 60, 1627–1632.

Rawls, J.F., Johnson, S.L., 2000. Zebrafish kit mutation reveals primary and secondary regulation of melanocyte development during fin stripe regeneration. Development 127, 3715–3724.

Reynolds, L.P., Killilea, S.D., Redmer, D.A., 1992. Angiogenesis in the female reproductive system. FASEB J. 6, 886–892.

Risau, W., 1997. Mechanisms of angiogenesis. Nature 386, 671–674.

Santamaria, J.A., Mari-Beffa, M., Santos-Ruiz, S., Becerra, J., 1996. Incorporation of Bromodeoxyuridine in regenerating fin tissue of the gold fish *Carassius auratus*. J. Exp. Zool. 275, 300–307.

Shi, Q., Raffi, S., Wu, M.H.D., Wijelath, E.S., Yu, C., Ishida, A., Fujita, Y., Kothari, S., Mohler, R., Sauvage, L.R., Moore, M.A.S., Storb, R.F., Hammond, W.P., 1998. Evidence for circulating bone marrow-derived endothelial cells. Blood 92, 362–367.

Westerfield, M., 1993. The Zebrafish Book. University of Oregon Press, Eugene, OR.